Theory of spontaneous emission in an optical cavity

Ichiro Takahashi and Kikuo Ujihara

The University of Electro-Communications, 1-5-1 Chofugaoka, Chofu, Tokyo 182, Japan

Spontaneous emission in a one-dimensional Fabry-Pérot-type optical cavity is analyzed quantum mechanically. Via a monolayer dielectric cavity model, expressions describing the atomic-location dependence of the emission intensities and the spectra observed on both sides of the cavity are obtained. The probability amplitude for the upper atomic state is analyzed and its time-evolution equation is given. The probability amplitude is shown to be proportional to ''the electric field amplitude for a single emission event'' introduced classically by Huang *et al.* [Appl. Phys. Lett. **61**, 2961 (1992)]. An expression for the emission spectrum applicable to a general one-dimensional cavity structure is obtained. [S1050-2947(97)04509-5]

PACS number(s): 42.60.−v

I. INTRODUCTION

It has been demonstrated theoretically [1,2] and experimentally [3–8] that spontaneous emission, which had been believed to be an inherent nature of the atom, can be modified in a cavity comparable in size to the wavelength of light emitted. The modification includes enhancement and inhibition of spontaneous emission in a cavity, which stem from the alteration of the vacuum field mode structure from that of free space. These effects are accounted for by considering the interaction between an atom and cavity modes. In the strong coupling regime, where a two-level atom is coupled to a single cavity mode of a high-Q cavity, spontaneous emission can even be reversible [9,10]. From an engineering viewpoint, controlling the spontaneous emission in such a cavity (microcavity) is of considerable interest because it suggests the possibility of optical devices such as a laser with an extremely low threshold due to the high coupling ratio of the emission into a lasing mode. Accordingly the spontaneous emission in the cavity is crucial for realizing such a device as a semiconductor microcavity laser, and has been investigated both theoretically and experimentally by a number of authors [11–17].

Spontaneous emission by a two-level atom in a Fabry-Pérot-type cavity constitutes the basis for cavity QED, and has been studied theoretically by many authors [18–24]. In particular, a theory of the emission intensity and the spectrum observed outside the cavity is of great interest because the experimental verification of the theory is straightforward. For example, De Martini *et al.* [22] have obtained expressions for the spontaneous emission rates for different active-dipole orientations and cavity configurations using the quantized radiation field with the three-dimensional traveling-wave modes of the cavity. They showed the spontaneous emission pulse shape detected outside the cavity to be generally nonexponential. Huang *et al.* [25] have derived an expression for the spectrum of spontaneous emission from a GaAs quantum well localized in an $Al_xGa_{1-x}As$ planar microcavity using a classical, one-dimensional theory. They showed that the intensity and the spectrum of spontaneous emission outside the cavity depend on the precise dipole position, and each of these differs on the two sides of the cavity. Both the intensities and emission spectra were measured

on the two sides of the cavity and excellent agreement was found between theory and experiment. However, their ''electric field amplitude for a single emission event'' was left as an unknown function. Although Deppe *et al.* [26] considered that problem using the quantum-mechanical wave-packet approach and obtained the same expression for the emission spectrum, the emission spectrum from the dipole in the absence of cavity was not derived from first principles. Feng and Ujihara have derived in a strict way a delay-differential equation of the atomic state in a one-dimensional optical cavity with output coupling using mode functions with a continuous spectrum, and have demonstrated the time development of emission intensity observed outside the cavity as well as the enhancement and inhibition of spontaneous emission [20,21]. Recently, Gieβen *et al.* [27] have considered the propagation effects on the spontaneous emission by a two-level atom in a one-dimensional cavity with perfectly reflecting mirrors. They showed that the spontaneous emission always occurs first at the free space rate until the light reflected by the cavity mirrors returns to the atom, thus causing an abrupt change in further emission.

Motivated by earlier studies on microcavities, we analyze in this paper spontaneous emission in a one-dimensional cavity on the basis of the theory in Refs. [20,21]. Our main objective is to calculate the atomic-location dependence of the emission intensities and the spectra observed on both sides of the cavity. Our theory can be applied not only to a general one-dimensional cavity but also to a one-dimensional microcavity.

In this paper, we first calculate quantum mechanically the intensity of spontaneous emission and the spectrum observed outside a one-dimensional monolayer optical cavity, which in practice corresponds to a low Q cavity. The emission spectrum agrees with that of Haung *et al.* [25] and the quantum-mechanical counterpart of their ''electric field amplitude for a single emission event'' is given together with its time-evolution equation. A closed-form expression for the emission spectrum is obtained using the response function in the general sense [28], admittance. This expression can be applied to a cavity with a general one-dimensional structure.

In Sec. II we summarize the theory given in Ref. [21] for the quantum-mechanical formulation of the field. The interaction between a quantized field and a two-level atom in the

cavity is examined to yield a delay-differential equation for the atomic state. In Sec. III we derive expressions for the intensity and the spectrum observed outside the monolayer cavity, showing in general an asymmetric property of emissions to the right and to the left of the cavity. We also derive the expression for the quantum-mechanical counterpart of ''the electric field amplitude for a single emission event'' of Haung *et al.*, which is shown to be proportional to the probability amplitude of the upper atomic state. Furthermore we generalize the expression for the emission spectrum to obtain one that can be applied to an arbitrary one-dimensional cavity structure. Numerical examples for microcavities are presented in Sec. IV. A brief discussion and conclusions are given in Secs. V and VI, respectively.

II. SPONTANEOUS EMISSION IN THE CAVITY

We present the quantum-mechanical formulation of the atom-cavity system following the theory described in Ref. [21]. Figure 1 shows our one-dimensional model cavity, which comprises a dielectric slab extending in the region $-l < z < l$ with dielectric constant ε_1. The space outside is a vacuum with dielectric constant ε_0. The permeability μ is constant throughout the entire space. We impose a periodic boundary condition with a large period $2l + L$ in the z direction. The electric and magnetic fields are assumed to be di-
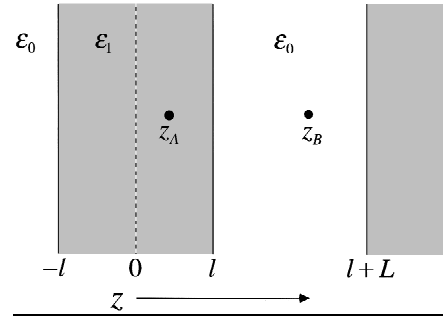

FIG. 1. The model cavity. The emitting atom is at z_A and the observing point is at z_B. The dielectric constants inside and outside the cavity are ε_1 and ε_0, respectively. A periodic boundary condition with a period $2l + L$ much larger than l is imposed on the mode function $U_j(z)$.

rected along the x and y axes, respectively. The velocities of light inside and outside the cavity are denoted by c_1 and c_0, respectively. The mode function of the jth mode describing the spatial distribution of the field is denoted by $U_j(z)$. It can be shown that there exist two kinds of orthonormal mode functions $U_j^a(z)$ and $U_j^b(z)$, differing in symmetry properties, to which we refer as the a and the b mode, respectively. In the limit $L \to \infty$, both modes are degenerate and continuous, and the mode density is $\rho = L/2\pi c_0$ for each a and b mode. The mode functions read

$$U_j^a(z) = \alpha_j \times \begin{cases} \sin(k_{j1}z) & (|z| < l) \\ \sin(k_{j1}l)\cos[k_{j0}(z-l)] + \dfrac{c_0}{c_1}\cos(k_{j1}l)\sin[k_{j0}(z-l)] & (l < z < l+L), \end{cases} \tag{2.1a}$$

$$U_j^b(z) = \beta_j \times \begin{cases} \cos(k_{j1}z) & (|z| < l) \\ \cos(k_{j1}l)\cos[k_{j0}(z-l)] - \dfrac{c_0}{c_1}\sin(k_{j1}l)\sin[k_{j0}(z-l)] & (l < z < l+L). \end{cases} \tag{2.1b}$$

Here $k_{ji} = \omega_j/c_i$ $(i=0,1)$, where ω_j is the frequency of the $j$the mode. It can be shown that the mode functions $U_j(z)$ and $dU_j(z)/dz$ are, respectively, mutually orthogonal in one period $2l + L$. The constants α_j and β_j are obtained by normalizing the mode functions with $\varepsilon(z)$ as the weighting factor:

$$\alpha_j^2 = \frac{2}{\varepsilon_1 L} \frac{1}{1 - K\sin^2(k_{j1}l)}, \tag{2.2a}$$

$$\beta_j^2 = \frac{2}{\varepsilon_1 L} \frac{1}{1 - K\cos^2(k_{j1}l)}, \tag{2.2b}$$

where $K = 1 - (\varepsilon_0/\varepsilon_1)$. They can be expanded in Fourier series as

$$\alpha_j^2 = \frac{2}{\varepsilon_1 L} \frac{2c_0}{c_1} \sum_{n=0}^{\infty} \frac{(-r)^n}{1+\delta_{0,n}} \cos(2nk_{j1}l), \tag{2.3a}$$

$$\beta_j^2 = \frac{2}{\varepsilon_1 L} \frac{2c_0}{c_1} \sum_{n=0}^{\infty} \frac{r^n}{1+\delta_{0,n}} \cos(2nk_{j1}l). \tag{2.3b}$$

Here, $r[=(c_0-c_1)/(c_0+c_1)]$ is the amplitude reflectivity at the interfaces as seen from inside the cavity and δ is the Kronecker delta. The parameters characterizing the cavity are given as follows:

$$\omega_m^a = \omega_c(2m+1), \quad \omega_m^b = 2m\omega_c \quad (m=0,1,2,3,\ldots)$$

$$\gamma_c = \frac{\omega_c}{\pi} \ln\left(\frac{1}{r}\right), \tag{2.4}$$

$$\omega_c = \frac{2\pi}{t_r} = \frac{\pi c_1}{2l},$$

where ω_m^a and ω_m^b are resonant frequencies for a and b modes, respectively, γ_c is the cavity decay constant (or half-

width of the resonant mode), ω_c is the mode separation, and t_r is the round-trip time in the cavity ($=4l/c_1$).

We follow the quantization procedure for the free field using the orthogonality of the mode functions and consider the spontaneous emission process by a two-level atom located at z_A with transition frequency ω_A [21]. The Hamiltonian of the atom-field system can be written as

$$\hat{H} = \sum_j \hbar \omega_j \hat{a}_j^\dagger \hat{a}_j + \hat{H}_A - \hat{\mu}\hat{E}(z_A) = \sum_j \hbar \omega_j \hat{a}_j^\dagger \hat{a}_j + \hat{H}_A$$
$$- i \sum_j \left(\frac{\hbar \omega_j}{2}\right)^{1/2} U_j(z_A) \hat{\mu}[\hat{a}_j - \hat{a}_j^\dagger], \quad (2.5)$$

where $\hat{H}_A$ is the atomic Hamiltonian, $\hat{E}$ is the electric field operator, and $\hat{a}_j$ and $\hat{a}_j^\dagger$ are the annihilation and creation operators, respectively, for the jth mode. An electric dipole interaction is assumed with $\hat{\mu}$ being the x component of the electric dipole operator of the atom, and a dipole approximation is made. The system wave function in the Schrödinger picture is of the form

$$|\psi(t)\rangle = C_u(t)|u\rangle|0\rangle e^{-i\omega_A t} + \sum_j C_{lj}(t)|l\rangle|1_j\rangle e^{-i\omega_j t}. \quad (2.6)$$

Here, $|u\rangle|0\rangle$ denotes the state for which atom is at the upper state and no photon exists in any mode; $|l\rangle|1_j\rangle$ denotes the state for which the atom is at the lower state and one photon exists in mode j while no photon exists in all the other modes. $C_u(t)$ and $C_{lj}(t)$ are the probability amplitudes for the states $|u\rangle|0\rangle$ and $|l\rangle|1_j\rangle$, having initial conditions $C_u(0)=1$ and $C_{lj}(0)=0$, respectively. The Schrödinger equation with Eqs. (2.5) and (2.6) yields the following coupled equations of motion for the probability amplitudes:

$$\dot{C}_u(t) = -\sum_j \left(\frac{\omega_j}{2\hbar}\right)^{1/2} U_j(z_A) \mu_A e^{-i(\omega_j - \omega_A)t} C_{lj}(t), \quad (2.7)$$

$$\dot{C}_{lj}(t) = \left(\frac{\omega_j}{2\hbar}\right)^{1/2} U_j(z_A) \mu_A^* e^{i(\omega_j - \omega_A)t} C_u(t), \quad (2.8)$$

where μ_A is the x component of the dipole matrix element and the dot indicates the time derivative. Eliminating C_{lj} using $C_{lj}(0)=0$, we have

$$\dot{C}_u(t) = -\frac{|\mu_A|^2}{2\hbar} \sum_j \omega_j U_j^2(z_A) \int_0^t e^{i(\omega_j - \omega_A)(t'-t)} C_u(t') dt'. \quad (2.9)$$

The above equation can be rewritten as

$$\dot{C}_u(t) = -\frac{\omega_A |\mu_A|^2}{2\hbar} \int_0^t dt' \int_{-\infty}^\infty d\omega_j \rho(\omega_j) \{[U_j^a(z_A)]^2$$
$$+ [U_j^b(z_A)]^2\} e^{i(\omega_j - \omega_A)(t'-t)} C_u(t'). \quad (2.10)$$

Here in the second integral we have replaced the summation Σ_j by an integral with the mode density and the lower limit zero by negative infinity. The factor ω_j has been taken out of the integral as a constant ω_A since the spectrum of $e^{-i\omega_A t} C_u(t)$ has a highly peaked value at ω_A. Substituting the mode functions for $|z| < l$ in Eqs. (2.1a) and (2.1b) into (2.10), and using Eq. (2.3), we obtain a delay differential equation for $C_u(t)$:

$$\dot{C}_u(t) = -\frac{A_0}{2}\Bigg[C_u(t)H(t) + 2\sum_{n=1}^\infty r^{2n} e^{i\omega_A n t_r} C_u(t-nt_r)$$
$$\times H(t-nt_r) + \sum_{n=0}^\infty r^{2n+1} e^{i\omega_A(nt_r+t_1)} C_u(t-nt_r-t_1)$$
$$\times H(t-nt_r-t_1) + \sum_{n=0}^\infty r^{2n+1} e^{i\omega_A(nt_r+t_2)}$$
$$\times C_u(t-nt_r-t_2)H(t-nt_r-t_2)\Bigg], \quad (2.11)$$

where

$$t_1 = \frac{2(l-z_A)}{c_1}, \quad t_2 = \frac{2(l+z_A)}{c_1} = t_r - t_1. \quad (2.12)$$

$H(t)$ is the unit step function and $A_0 (= \eta^2 \omega_A |\mu_A|^2/\hbar\varepsilon_0 c_0)$ is the spontaneous emission rate in a one-dimensional free space of dielectric constant ε_1. In the above expression for A_0, the effect of a medium in which the atom is embedded on the spontaneous emission rate is included in the local field correction factor denoted by η [29]. Equation (2.11) describes the interaction of the emitted photon with the emitting atom with correct delay times corresponding to the distance traveled by the photon before coming back to the atom. If we assume, for example, $0 < t < t_1 < t_2$, then all summation terms vanish and Eq. (2.11) reduces to a simple form $\dot{C}_u(t) = -(A_0/2)C_u(t)H(t)$. Obviously this equation states that the upper atomic population decays exponentially at the free space rate A_0 until the reflected light returns to the atom at t_1 [20,21]. Equation (2.11) determines the decay of the atom completely and its numerical solution will be presented in Sec. IV.

III. EMISSION INTENSITY AND SPECTRUM

The observable field intensity is the quantum-mechanical average of the product of the negative and the positive frequency parts of the electric field operator, $\hat{E}^{(-)}$ and $\hat{E}^{(+)}$ [32], which are given by

$$\hat{E}^{(+)}(z) = [\hat{E}^{(-)}(z)]^\dagger = i\sum_j \left(\frac{\hbar\omega_j}{2}\right)^{1/2} U_j(z)\hat{a}_j. \quad (3.1)$$

Then the field intensity at $z_B (>l)$ has the form [20]

$$\langle\psi(t)|\hat{E}^{(-)}(z_B)\hat{E}^{(+)}(z_B)|\psi(t)\rangle=\left|\frac{\mu_A^*}{2}\int_0^t dt'\,C_u(t')\sum_j\,\omega_j[U_j^a(z_A)U_j^a(z_B)+U_j^b(z_A)U_j^b(z_B)]e^{-i(\omega_j-\omega_A)(t-t')}\right|^2. \quad (3.2)$$

We note that the quantity in the absolute square is proportional to the integral transform of $C_u(t)$ by the kernel that is given by the summation in the integrand and contains the effect of the cavity on the observable field [33].

Here we define the following characteristic times:

$$t_R=-\frac{z_A-l}{c_1}+\frac{z_B-l}{c_0}, \quad t_L=\frac{t_r}{2}+\frac{z_A+l}{c_1}+\frac{z_B-l}{c_0} \quad (z_B>l),$$
$$(3.3)$$

where t_R is the time required for the light to travel rightward from the atom to z_B, and t_L is the time required to travel to the left interface and then to the observation point z_B. Using the mode functions in Eqs. (2.1) with normalization constants in Eq. (2.3) and replacing the summation by an integral, we can calculate Eq. (3.2) to obtain [34]

$$\langle\psi(t)|\hat{E}^{(-)}(z_B)\hat{E}^{(+)}(z_B)|\psi(t)\rangle$$
$$=\frac{\omega_A^2|\mu_A|^2}{4\varepsilon_0\varepsilon_1 c_0 c_1}(1-r^2)|f(z_A,z_B,t)|^2, \quad (3.4)$$

where

$$f(z_A,z_B,t)=e^{-i\omega_A t}\left[\sum_{n=0}^{\infty}r^{2n}e^{i\omega_A(nt_r+t_R)}C_u(t-nt_r-t_R)\right.$$
$$\times H(t-nt_r-t_R)+\sum_{n=0}^{\infty}r^{2n+1}e^{i\omega_A(nt_r+t_L)}$$
$$\left.\times C_u(t-nt_r-t_L)H(t-nt_r-t_L)\right] \quad (z_B>l).$$
$$(3.5)$$

Equation (3.4) together with (3.5) shows that the observable field intensity at z_B and t results from a superposition of probability waves emitted by the atom at $t-(nt+t_R)$ and $t-(nt_r+t_L)$ with amplitudes proportional to C_u at those times, showing the effect of multiple reflection at interfaces on the emission process. The field intensity at $z_B<-l$ can be obtained from Eqs. (3.4) and (3.5) by replacing both z_A and z_B by $-z_A$ and $-z_B$ in Eqs. (3.3), respectively.

If we assume for the moment that the function $f(z_A,z_B,t)$ represents a classical wave and $C_u(t)$ a classical amplitude, then we can calculate the power spectrum of the emission on a purely classical ground. A quantum-mechanical justification for this procedure will be given later in this section. To find the power spectrum that is proportional to the absolute square of the Fourier transform of the "field amplitude" $f(z_A,z_B,t)$, we define $D(t)=e^{-i\omega_A t}C_u(t)H(t)$ and write its Fourier transform as $D(\omega)$. The term of, for example, $e^{-i\omega_A t}r^{2n}e^{i\omega_A(nt_r+t_R)}C_u(t-nt_r-t_R)H(t-nt_r-t_R)$ is transformed to $r^{2n}e^{i\omega(nt_r+t_R)}D(\omega)$. Then the spectrum corresponding to Eq. (3.4) becomes inde-

pendent of z_B but dependent on z_A, as seen by the z_A and z_B dependence of t_R and t_L. Thus we can write the spectrum in the form

$$S(z_A,\omega)=\frac{\omega_A^2|\mu_A|^2}{4\varepsilon_0\varepsilon_1 c_0 c_1}T|D(\omega)|^2$$
$$\times\left\{\frac{1+R+2\sqrt{R}\,\cos\{2\omega[(z_A+l)/c_1]\}}{1+R^2-2R\,\cos(4\omega l/c_1)}\right\}$$
$$(z_B>l), \quad (3.6)$$

where $R=r^2$ and $T=1-R$. If the observation point is located to the left of the cavity, $z_B<-l$, the factor z_A+l should be replaced by $-z_A+l$. This equation is of the same form as that derived classically in Ref. [25] and explicitly shows the dependence of the power spectrum on the atomic location z_A.

We note that $D(t)$, which is a product of a carrier wave of frequency ω_A and an upper atomic state probability amplitude $C_u(t)$, is of quantum-mechanical origin and represents the probability amplitude in the form of a wave packet going back and forth in the cavity and is the quantum-mechanical counterpart of ''the electrical field amplitude for a single emission event'' of Huang $et\ al.$ [25]. Note also that Eq. (2.11), or Eq. (2.10), determines $D(t)$ completely, while it remains as an unknown function in the classical, intuitive theory of Huang $et\ al.$

In the expression for the emission spectrum Eq. (3.6), we note that the term in curly braces represents the effect of multiple reflection at interfaces on the field outside the cavity. In other words, that term can be regarded as the response of the space to a source inside the cavity. If we define the admittance $Y(z_B,z_A,\omega)$ as the expectation value of the steady state electric field operator at z_B due to a classical unit point current source (polarized in the x direction) located at z_A with frequency ω [28], then the explicit expression of admittance for the monolayer model is given by

$$Y(z_B,z_A,\omega)=-\frac{1+r}{2\varepsilon_1 c_1}\left\{\frac{1+r\,\exp\{i2\omega[(z_A+l)/c_1]\}}{1-r^2\exp[i(4\omega l/c_1)]}\right\}$$
$$\times e^{i\omega t_R} \quad (z_B>l). \quad (3.7)$$

We can obtain the admittance for $z_B<-l$ by replacing z_A and z_B by $-z_A$ and $-z_B$, respectively. Comparing Eq. (3.6) with the absolute square of Eq. (3.7), we see that the emission spectrum for a monolayer cavity is proportional to the absolute square of the admittance. Thus we can express the emission spectrum Eq. (3.6) in terms of the admittance:

$$S(z_A,\omega)=\omega_A^2|\mu_A|^2|D(\omega)|^2|Y(z_B,z_A,\omega)|^2. \quad (3.8)$$

This equation shows that the emission spectrum observed outside the cavity is proportional to the product of the spec-

trum corresponding to the atomic motion in the cavity and the absolute square of admittance.

We have obtained Eq. (3.8) heuristically for a monolayer cavity. However, we can easily show that this equation, expressing the observable field intensity in terms of the admittance, applies to a general structure: The field intensity in Eq. (3.2) can also be written as

$$\langle \psi(t)|\hat{E}^{(-)}(z_B)\hat{E}^{(+)}(z_B)|\psi(t)\rangle$$

$$= \left| \sum_j \frac{\omega_j}{2} \mu_A^* U_j(z_A) U_j(z_B) \right.$$

$$\left. \times e^{-i(\omega_j - \omega_A)t} \int_0^t D(t')e^{i\omega_j t'} dt' \right|^2$$

$$= \omega_A^2 |\mu_A|^2 \left| \int_{-\infty}^{\infty} Y(z_B, z_A, \omega)D(\omega)e^{-i\omega t}d\omega \right|^2, \quad (3.9)$$

where ω_j has been factored outside the summation as ω_A because $D(\omega)$ has a highly peaked value at ω_A. The integral over ω comes from the Fourier transform of $D(t')$. Note that the field amplitude given by the last integral is in the form of the inverse Fourier transform of $Y(z_B, z_A, \omega)D(\omega)$. Thus it follows from Eq. (3.9) that the expression for the emission spectrum Eq. (3.8) holds for a general structure. The above discussion leading to Eq. (3.9) can be considered a quantum-mechanical justification for the procedure of obtaining the power spectrum, Eq. (3.6).

Our main results of the present paper include Eqs. (3.4)–(3.6), and their generalization Eqs. (3.8) and (3.9). Another result is that $D(t) = e^{-i\omega_A t}C_u(t)H(t)$ corresponds to the classical ''unknown function'' of Huang *et al.*

To gain the physical meaning of numerical results in the next section, let us now consider the decay process of the atom Eq. (2.9) and obtain approximate solutions for a single-resonant-mode limit of the monolayer cavity, where only the resonant mode ω_m^a (mth a mode) contributes appreciably to the interaction with the atom [21]. To this end we denote by $\mathcal{D}(s)$ the Laplace transform of $D(t) = e^{-i\omega_A t}C_u(t)H(t)$, multiply Eq. (2.9) by $e^{-i\omega_A t}$, and take the Laplace transform with the initial condition $D(0) = 1$. The result is given by

$$\mathcal{D}(s) \cong \frac{1}{s + i\omega_A - \varepsilon_1 c_1 A_0 Y(z_A, z_A, is)}, \quad (3.10)$$

where ω_j has been factored outside the summation as a constant frequency ω_A in Eq. (2.9). Evaluating the admittance at the location of the atom with the help of Eqs. (2.4), (2.12), and the single-resonant-mode conditions [21]

$$A_0 \ll 1/t_r, \quad \gamma_c \ll \omega_c \ll \omega_m^a, \quad \omega_m^a \cong \omega_A, \quad (3.11)$$

and substituting into Eq. (3.10), we obtain

$$\mathcal{D}(s) \cong \frac{s + i\omega_A + \gamma_c}{(s + i\omega_A + \gamma_c/2)^2 - (\gamma_c/2)^2 + (\Omega/2)^2}, \quad (3.12)$$

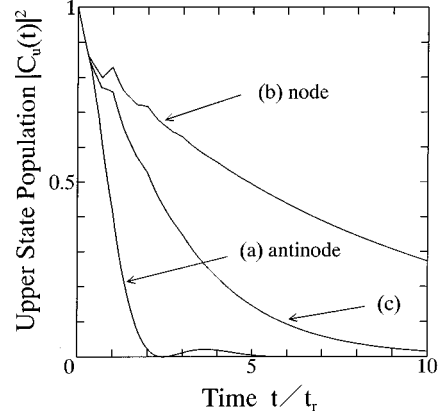where Ω is the vacuum Rabi frequency given by [21]

FIG. 2. Time evolution of the upper-state population for a low-Q cavity: $|C_u(t)|^2$ vs t/t_r, where t_r is the round-trip time in the cavity. The atom is set at (a) an antinode ($z_A/l=0.2$), (b) a node ($z_A/l=0.4$), and (c) a position ($z_A/l=0.35$) between the node and the antinode. $2l/\lambda=2.5$ ($\omega_A=\omega_m^a=5\omega_c$), $r=0.6$, and $t_r A_0=0.5$ for curves (a), (b), and (c).

$$\left(\frac{\Omega}{2}\right)^2 \cong \frac{\omega_c A_0}{\pi} \sin^2(\omega_m^a t_A), \quad (3.13)$$

and $t_A = z_A/c_1$. For an underdamped cavity $\gamma_c \ll \Omega$, we can easily find the inverse Laplace transform of Eq. (3.12):

$$D(t) \cong e^{-i\omega_A t}e^{-\gamma_c t/2}\cos\left(\frac{\Omega}{2}t\right). \quad (3.14)$$

In the same manner, for an overdamped cavity $\gamma_c \gg \Omega$, the inverse operation yields

$$D(t) \cong e^{-i\omega_A t}e^{-\Omega^2 t/4\gamma_c}. \quad (3.15)$$

Equations (3.14) and (3.15) agree with Eqs. (3.18) and (3.19) in Ref. [21], respectively.

Numerical examples will be presented in the next section, with emphasis on the atomic-location dependence of the emission intensities and the spectra observed on both sides of the cavity.

IV. NUMERICAL EXAMPLES

In this section, we present some numerical examples based on the theory developed so far. Our main concern here is the atomic-location dependence of the emission intensity and the spectrum observed on both sides of monolayer microcavities. Figures illustrated here include the time evolution of the upper state population of the atom $|C_u(t)|^2$ calculated from the delay differential equation Eq. (2.11), the spectrum $|D(\omega)|^2$ calculated from the Fourier transform of $D(t) = e^{-i\omega_A t}C_u(t)H(t)$, the absolute square of the admittance at z_B, $|Y(z_B, z_A, \omega)|^2$, calculated from Eq. (3.7), and the emission spectrum as a quantity proportional to the product of $|D(\omega)|^2$ and $|Y(z_B, z_A, \omega)|^2$.

Figure 2 shows the time evolution of the upper state population $|C_u(t)|^2$ vs the scaled time t/t_r for a 2.5λ cavity where λ is the wavelength in the cavity and the atom is located at an antinode ($z_A/l=0.2$) [curve (a)], a node ($z_A/l=0.4$) [curve (b)], and a position ($z_A/l=0.35$) between the node

and the antinode of the cavity resonant mode [curve (c)]. Other parameters include the amplitude reflectivity $r = 0.6$ and the spontaneous emission rate $A_0 = 0.5/t_r$ in the free space of dielectric constant ε_1. The curve (a) shows a fast decay with a very weak Rabi oscillation. From Eqs. (2.4) and (3.14), this corresponds to the cavity decay constant $\gamma_c = 0.16\omega_c$ and the Rabi frequency $\Omega = 0.32\omega_c$. Thus the conditions for the single resonant mode limit for an underdamped cavity are roughly satisfied. When the atom is located at the node, as shown in curve (b), the atomic decay is quite slow compared with curve (a) and the spontaneous emission is substantially suppressed. In this case the approximate solution Eq. (3.13) yields the zero Rabi frequency because $\sin(\omega_m^a t_A) = 0 (m=2)$, and the upper state population remains a constant equal to unity from Eq. (3.15). However, the slow decay indicates that other modes in which the atom may be near or just at an antinode contribute to the emission [20]. When the atom is located between the node and the antinode, the atom-field coupling is medium and the decay curve lies between the curves (a) and (b), as shown in (c). Abrupt changes in the curves indicate the counteraction of reflected radiations on the atom. In particular, a closer look at the figure shows that the first interactions of the atom with the reflected radiations for curves (a), (b), and (c) occur at $t = 0.4t_r$, $0.3t_r$, and $0.325t_r$, respectively, which are consistent with Eq. (2.11).

Figure 3(a) shows the spectrum $|D(\omega)|^2$ corresponding to the atomic curve (a) in Fig. 2. The spectrum is symmetric about the atomic transition frequency ω_A and displays two peaks at $\omega \cong \omega_A \pm 0.16\omega_c$ reflecting the Rabi oscillation of $|C_u(t)|^2$ with frequency $\Omega = 0.32\omega_c$. Other numerical results (not shown here) indicate that when the atom is at a node or at an antinode of a resonant cavity where the cavity length is an integral multiple of the half wavelength of light, the spectrum $|D(\omega)|^2$ is almost symmetric about ω_A. The same is true of the admittance spectrum $|Y(z_B, z_A, \omega)|^2$.

The absolute square of the admittance $|Y(z_B, z_A, \omega)|^2$ versus $(\omega - \omega_A)/\omega_c$ for outside the monolayer cavity is shown in Fig. 3(b) for the case where z_A is at the antinode. The solid and the dashed curves are for $z_B > l$ and $z_B < -l$, respectively. It can be shown from Eq. (3.7) that for a resonant cavity, $|Y(z_B, z_A, \omega)|^2$ has the same value for $z_B > l$ and $z_B < -l$ at a resonant frequency where $(\omega - \omega_A)/\omega_c$ is an integer. In fact the figure shows that at resonant frequencies the admittances (for $z_B > l$ and for $z_B < -l$) have the same value while in the frequency region between the resonant frequencies they are different. In particular we note that in the frequency region near the atomic transition frequency ω_A, the admittance spectra for $z_B > l$ and for $z_B < -l$ almost coincide. In this case we can expect symmetric emission spectra with respect to $z_B > l$ and $z_B < -l$, since the emission spectrum is proportional to $|D(\omega)|^2 |Y(z_B, z_A, \omega)|^2$ in which $D(\omega)$ is independent of the observation point (more explicit conditions for symmetric emission spectra will be given later).

The emission spectra corresponding to curve (a) in Fig. 2 are shown in Fig. 3(c). The spectrum is proportional to the product of spectra $|D(\omega)|^2$ in Fig. 3(a) and $|Y(z_B, z_A, \omega)|^2$ in Fig. 3(b). The solid and dashed curves are for $z_B > l$ and $z_B < -l$, respectively, as before. As can be seen from the figure the solid and dashed curves almost coincide, showing
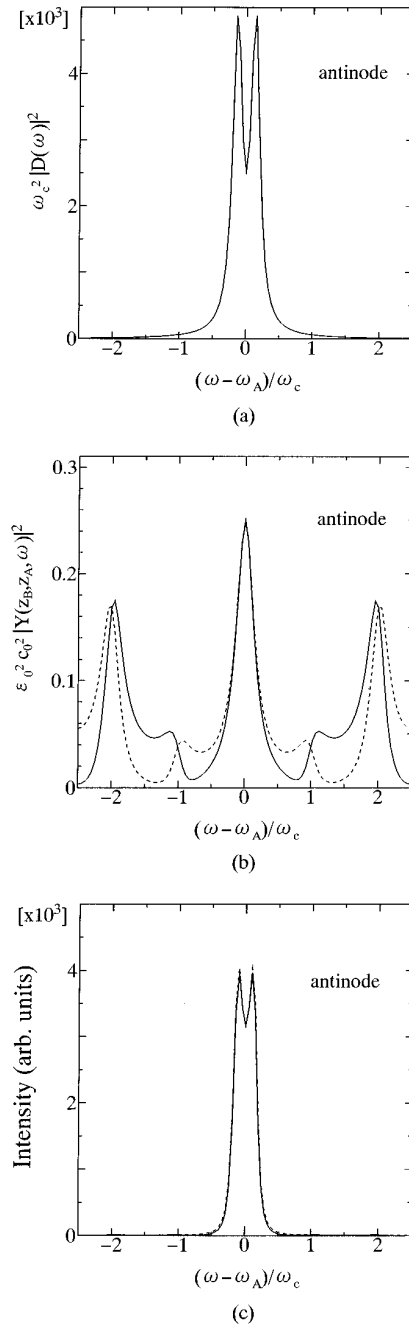

FIG. 3. Spectrum of $D(t)$ and the emission spectra observed outside the cavity corresponding to curve (a) in Fig. 2, where the atom is at an antinode ($z_A/l = 0.2$). The spectra of $Y(z_B, z_A, \omega)$ are also shown. (a) Spectrum of $D(t)$: $\omega_c^2 |D(\omega)|^2$ vs $(\omega - \omega_A)/\omega_c$. Two peaks at $\omega \cong \omega_A \pm 0.16\omega_c$ correspond to the Rabi oscillation of $|C_u(t)|^2$ with $\Omega = 0.32\omega_c$. (b) Admittance spectrum: $\varepsilon_0^2 c_0^2 |Y(z_B, z_A, \omega)|^2$ vs $(\omega - \omega_A)/\omega_c$. The solid and the dashed curves represent the spectra observed on the right ($z_B > l$) and on the left ($z_B < -l$) side of the cavity, respectively. (c) Emission spectrum proportional to the product of spectra in (a) and (b), showing almost symmetric emission. The solid and the dashed curves are the spectra observed on the right ($z_B > l$) and on the left ($z_B < -l$) side of the cavity, respectively.

symmetric radiations to the right and to the left of the cavity ($z_B > l$ and $z_B < -l$), as mentioned above.

Figure 4 shows the spectra corresponding to the curve (b) in Fig. 2 where the atom is located at the node. The figure
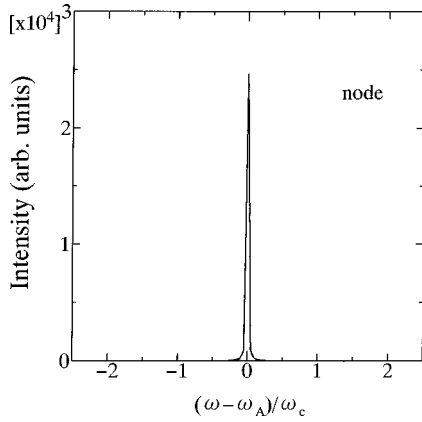
FIG. 4. Emission spectra corresponding to curve (b) in Fig. 2, where the atom is at a node ($z_A/l = 0.4$). The solid and the dashed curves are the spectra observed on the right ($z_B > l$) and on the left ($z_B < -l$) side of the cavity, respectively, showing symmetric emission spectra.

shows almost identical radiations to the right and to the left of the cavity. Since the atomic decay is quite slow, the corresponding spectrum $|D(\omega)|^2$ is highly peaked at ω_A, where the admittances have the same value, as stated earlier. Thus we have symmetric emission spectra ($z_B > l$ and $z_B < -l$).

When the atom is located between the node and the antinode, i.e., $z_A/l = 0.35$, as shown in Fig. 5, we have slightly asymmetric emission spectra for $z_B > l$ and for $z_B < -l$ due to the difference in admittance spectra near ω_A. The spectra are highly peaked at ω_A and are similar to those of Fig. 4, because the atomic location ($z_A/l = 0.35$) is close to the node ($z_A/l = 0.4$) where the atom-field coupling is quite weak.

The differences in the emission spectra in Figs. 3(c), 4, and 5 show an example of the fact that the emission spectrum depends on the atomic location. The numerical results including those not shown in this paper suggest that the emission spectra for our monolayer cavity are symmetric if, roughly speaking, the following conditions are satisfied. (1) The cavity length is an integral multiple of the half wavelength of light. (2) The atomic location is at a node or at an
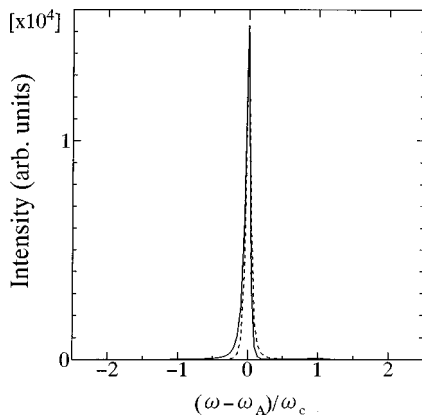

FIG. 5. Emission spectra corresponding to curve (c) in Fig. 2, where the atom is located at $z_A/l = 0.35$ between the node ($z_A/l = 0.4$) and the antinode ($z_A/l = 0.2$). The solid and the dashed curves are the spectra observed on the right ($z_B > l$) and on the left ($z_B < -l$) side of the cavity, respectively, showing slightly asymmetric emission spectra.

FIG. 6. Emission spectra for a nonresonant cavity where $2l/\lambda = 2.2$, $r = 0.6$, $t_r A_0 = 0.5$, and $z_A/l = 0.4$. The solid and the dashed curves are the spectra observed on the right ($z_B > l$) and on the left ($z_B < -l$) side of the cavity, respectively, showing asymmetric emission spectra.
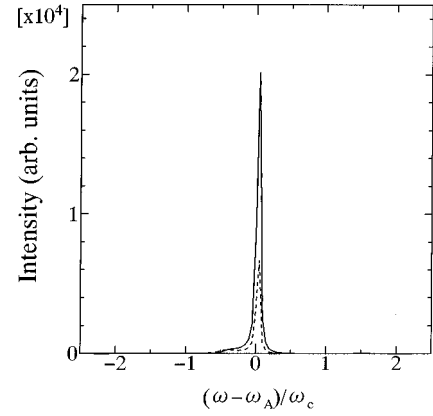
antinode of the cavity resonant mode. (3) The linewidth of the spectrum $|D(\omega)|^2$ is much smaller than the atomic transition frequency ω_A.

Emission spectra for a nonresonant cavity are illustrated in Fig. 6, where $2l/\lambda = 2.2$, $z_A/l = 0.4$, and other parameters are the same as those for $2l/\lambda = 2.5$. We observe that both the emission line shapes and the spectrally integrated intensities differ for $z_B > l$ and $z_B < -l$, showing asymmetric emission spectra. The differences arise essentially from the difference in $|Y(z_B, z_A, \omega)|^2$ in the frequency region close to $\omega = \omega_A$, since the resultant emission spectrum is proportional to $|D(\omega)|^2 |Y(z_B, z_A, \omega)|^2$, where $D(\omega)$ is independent of the observation point.

It should be noted that the sum of the energy radiated from both sides of the cavity should be a constant ($\hbar\omega_A$) independent of the atomic location. We have verified numerically that the sum is constant by calculating the spectrally integrated intensity, for cavities of lengths $2l = 1.35\lambda$, 1.5λ, 2.5λ, and 18.1λ.

V. DISCUSSION

In Secs. II and III we have made an approximation that the factor ω_j can be taken out of the summation or the integral as a constant frequency ω_A because the function in the summation or the integrand has a highly peaked spectrum at ω_A or several peaks near ω_A. This is equivalent to the condition that the atomic state varies much slower than the periodic motion of the light. This can be seen as follows: If the width $\Delta\omega_j$ of the spectrum is much smaller than ω_A, we have approximately $|\dot{C}_u(t)/C_u(t)| \sim A_0/2 \sim \Delta\omega_j \ll \omega_A$. This condition is satisfied even for a cavity with its length being of the order of the wavelength as well as for a conventional one, as discussed in Ref. [21].

In Sec. III we have derived the expressions for the field intensity and the spectrum observed outside the cavity. The following discussion will aid comparison between theory and experiment: Classically the spontaneously emitted light from the cavity will be of the form of wave trains of finite length, each of which corresponds to a single emission and enters the detector at random. If N is the number of wave trains

entering the detector during the time interval $2T$ required for a measurement, then the mean intensity I is proportional to the integral of the Fourier component $S_C(z_A, \omega)$ of a single wave train and is given by [35]

$$I = \frac{N}{2T} \int_{-\infty}^{\infty} S_C(z_A, \omega) d\omega. \qquad (5.1)$$

The $S_C(z_A, \omega)$ may be replaced in our case by the function $S(z_A, \omega)$ in Eq. (3.6). It follows from this consideration that we can obtain an expression for the measurable mean intensity using $S(z_A, \omega)$, and that this $S(z_A, \omega)$ exactly reproduces the steady state observed spectrum.

We have seen that $D(t) = e^{-i\omega_A t} C_u(t) H(t)$ is the quantum-mechanical counterpart of ''the electric field amplitude for a single emission event'' of Huang *et al.* Indeed $D(t)$ may be loosely regarded as ''a wave packet for a single emission'' from the atom at t with the envelope equal to the upper atomic state probability amplitude $C_u(t)$ in which the effects of multiple reflection and the interaction of reflected light with the atom are contained, as can be seen from the delay differential equation (2.11). Therefore our expression for the spontaneous emission spectrum observed outside the cavity (3.6) is of the same form as that derived classically by Huang *et al.* Our quantum-mechanical method, however, allows us to calculate the $D(t)$ from first principles without using experimental results.

Although the analysis presented in this paper is limited to one dimension, it can be served as an approximation to the situations in the three-dimensional world as has been seen by the work of Huang *et al.* [25]. If the cavity is a three-dimensional dielectric slab with the transverse dimensions much larger than the cavity length, there exist guided modes as well as longitudinal modes. Part of the radiation from the atom will couple to the guided modes resulting in guided waves along the transverse directions. Also, depending on the cavity length, there exist oblique resonant modes. The waves in these modes never return to the atom again, which would otherwise interact with the atom, causing kinks in the atomic decay process. Thus in a three-dimensional case we expect less kinky character in the time evolution of upper atomic population $|C_u(t)|^2$.

VI. CONCLUSIONS

In conclusions, we have analyzed in a consistent quantum-mechanical way the spontaneous emission in a monolayer optical cavity following closely the theory described in Ref. [21]. We have derived expressions for the intensity and the spectrum of spontaneous emission observed outside the cavity. The emission spectrum derived is of the same form as that given classically by Huang *et al.* In particular, we have shown that the probability amplitude for the upper atomic state is proportional to their ''electric field amplitude for a single emission event.'' We have also shown that the spontaneous emission intensities as well as the spectra are dependent on the atomic location, and that the emissions to the right ($z_B > l$) and to the left ($z_B < -l$) are in general asymmetric. This asymmetry for the monolayer cavity stems from that of admittance. We have given an expression for the emission spectrum applicable to a general one-dimensional cavity structure.

[1] E. M. Purcell, Phys. Rev. **69**, 681 (1946).

[2] D. Kleppner, Phys. Rev. Lett. **47**, 233 (1981).

[3] K. H. Drexhage, in *Progress in Optics*, edited by E. Wolf (North-Holland, New York, 1974), Vol. 12.

[4] P. Goy, J. M. Raimond, M. Gross, and S. Haroche, Phys. Rev. Lett. **50**, 1903 (1983).

[5] R. G. Hulet, E. S. Hilfer, and D. Kleppner, Phys. Rev. Lett. **55**, 2137 (1985).

[6] W. Jhe, A. Anderson, E. A. Hinds, D. Meschede, L. Moi, and S. Haroche, Phys. Rev. Lett. **58**, 666 (1987).

[7] D. J. Heinzen, J. J. Childs, J. E. Thomas, and M. S. Feld, Phys. Rev. Lett. **58**, 1320 (1987).

[8] F. De Martini, G. Innocenti, G. R. Jacobovitz, and P. Mataloni, Phys. Rev. Lett. **59**, 2995 (1987).

[9] E. T. Jaynes and F. W. Cummings, Proc. IEEE **51**, 89 (1963).

[10] G. Rempe, H. Walther, and N. Klein, Phys. Rev. Lett. **58**, 353 (1987).

[11] E. Yablonovitch, Phys. Rev. Lett. **58**, 2059 (1987).

[12] E. Yablonovitch, T. J. Gmitter, and R. Bhat, Phys. Rev. Lett. **61**, 2546 (1988).

[13] H. Yokoyama and S. D. Brorson, J. Appl. Phys. **66**, 4801 (1989).

[14] S. D. Brorson, H. Yokoyama, and E. P. Ippen, IEEE J. Quantum Electron. **26**, 1492 (1990).

[15] Y. Yamamoto, S. Machida, and G. Björk, Phys. Rev. A **44**, 657 (1991).

[16] G. Björk, S. Machida, Y. Yamamoto, and K. Igeta, Phys. Rev. A **44**, 669 (1991).

[17] G. Björk and Y. Yamamoto, IEEE J. Quantum Electron. **27**, 2386 (1991).

[18] J. J. Sanchez-Mondragon, N. B. Narozhny, and J. H. Eberly, Phys. Rev. Lett. **51**, 550 (1983).

[19] R. J. Cook and P. W. Milonni, Phys. Rev. A **35**, 5081 (1987).

[20] X. P. Feng and K. Ujihara, IEEE J. Quantum Electron. **25**, 2332 (1989).

[21] X. P. Feng and K. Ujihara, Phys. Rev. A **41**, 2668 (1990).

[22] F. De Martini, M. Marroco, P. Mataloni, L. Crescentini, and R. Loudon, Phys. Rev. A **43**, 2480 (1991).

[23] Q. Deng and D. G. Deppe, Phys. Rev. A **53**, 1036 (1996).

[24] S. M. Dutra and P. L. Knight, Phys. Rev. A **53**, 3587 (1996).

[25] Z. Huang, C. Lei, D. G. Deppe, C. C. Lin, C. J. Pinzone, and R. D. Dupuis, Appl. Phys. Lett. **61**, 2961 (1992).

[26] D. G. Deppe, C. Lei, C. C. Lin, and D. L. Huffaker, J. Mod. Opt. **41**, 325 (1994).

[27] H. Gießen, J. D. Berger, G. Mohs, P. Meystre, and S. F. Yelin, Phys. Rev. A **53**, 2816 (1996).

[28] K. Ujihara, Phys. Rev. A **18**, 659 (1978).

[29] If the atom is located in a dielectric medium, the electric field at the location of the atom is different from the macroscopic electric field, hence leading to the modification of the spontaneous emission rate from its vacuum rate (local field correc-

tion). Glauber and Lewenstein [30] have obtained the local field correction factor η to be $[3\varepsilon/(2\varepsilon+1)]$ by considering the electric field inside an empty cavity embedded in a dielectric medium with relative dielectric constant ε. On the other hand, $\eta=[(\varepsilon+2)/3]$ has been derived from a microscopic calculation by Knoester and Mukamel [31]. In the present paper η^2 is the correction factor for the spontaneous emission rate.

[30] R. J. Glauber and M. Lewenstein, Phys. Rev. A **43**, 467 (1991).

[31] J. Knoester and S. Mukamel, Phys. Rev. A **40**, 7065 (1989).

[32] R. J. Glauber, Phys. Rev. **130**, 2529 (1963).

[33] L. Knöll, W. Vogel, and D.-G. Welsch, Phys. Rev. A **36**, 3803 (1987).

[34] In our one-dimensional world the field intensity in Eq. (3.4) has the dimension of $[(\text{V/m})^2][(\text{m}^2)^2]$, which has the extra factor of $[(\text{m}^2)^2]$. This discrepancy arises from the normalizing process of our one-dimensional mode functions. In the present paper, however, we regard Eq. (3.4) as the field intensity.

[35] M. Born and E. Wolf, *Principle of Optics*, 6th ed. (Pergamon, Oxford, 1980), Chap. 7.